Photoelectron Spectroscopy of a Carbene/Silylene/Germylene Series[†]

Anthony J. Arduengo, III,[*,‡] Hans Bock,[#] Han Chen,[*,|] Michael Denk,[*,▲]
David A. Dixon,[*,‡] Jennifer C. Green,[*,§] Wolfgang A. Herrmann,[⊥] Nancy L. Jones,[‡]
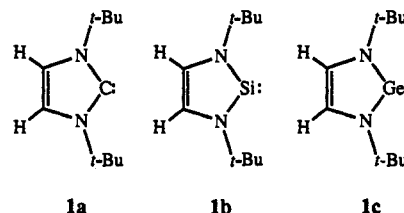Matthias Wagner,[§] and Robert West[▲]

*Contribution from the DuPont Science and Engineering Laboratory, Experimental Station,
P.O. Box 80328, Wilmington, Delaware 19898-0328, Anorganisch-chemisches Institut
der Johann Wolfgang Goethe-Universität, Marie-Curie-Strasse 1, Frankfurt, Germany,
Cray Research, Inc., 655 East Lone Oak Dr., Eagan, Minnesota 55121, Department of Chemistry,
University of Wisconsin, Madison, Wisconsin 53706, Inorganic Chemistry Laboratory,
Oxford University, South Parks Road, Oxford OX1 3QR, England, and Anorganisch-chemisches
Institut der Technischen Universität München, Lichtenbergstrasse 4,
D-W-8046 Garching, Germany*

Received April 5, 1994[⊛]

Abstract: The photoelectron spectra [HeI and He II] are reported for a carbene, a silylene, and a germylene (1,3-di-*tert*-butylimidazol-2-ylidene, 1,3-di-*tert*-butyl-1,3,2-diazasilol-2-ylidene, and 1,3-di-*tert*-butyl-1,3,2-diazagermol-2-ylidene). The experimental photoelectron spectra are assigned on the basis of predictions from density functional theory (DFT) calculations and first-order time-dependent perturbation theory. The predicted spectra agree well with the experimental ones both in ionization energy and band intensity. The carbene 1,3-di-*tert*-butylimidazol-2-ylidene is found to have a highest occupied molecular orbital (HOMO) that is essentially the in-plane lone pair of electrons at the carbene center (C σ-lp). The second ionization from the carbene occurs from a π-molecular orbital (π-3) that is largely the C=C double bond in the imidazole ring with some contributions from the nitrogens and the carbene center. The HOMOs of the silylene and germylene are derived from the π-3, orbital which changes character to become more concentrated on the two-coordinate main group IV center (Si or Ge) and less involved with the C=C double bond. The Si σ-lp and Ge σ-lp orbitals are subjacent and responsible for the second ionization bands. The molecular orbital structure and total electron distribution predicted from the DFT calculations are used to illustrate the differences in structure and chemistry in the carbene, silylene, and germylene compounds. The X-ray structure of 1,3-di-*tert*-butylimidazol-2-ylidene is also reported.

Introduction

The syntheses, isolation, and experimental determinations of the structures of a series of stable carbenes in the imidazol-2-ylidene family have prompted a number of studies addressing the electronic structure of these novel compounds.[1,2] Examples include the measurement of the electron density of the carbene by X-ray/neutron diffraction techniques[3] and the measurement of the chemical shift tensor of the carbene carbon.[4] Furthermore there has been significant synthetic interest in deriving the silylene and germylene analogs of the carbene to look at the effect of substituting silicon[5] and germanium[6] for the carbene carbon. A series of identically substituted compounds in this family (1a–c) has been prepared and is available for comparative studies.

1a   1b   1c

Although photoelectron spectroscopy is an important tool for studying the nature of the energetics of the electrons in a molecule, it has not been previously used to study the lighter main group IV element compounds in two-coordinate oxidation state II compounds. Herein we present a combined experimental and theoretical study of the photoelectron spectroscopy of these novel species. For the theoretical portion, we employ density functional theory (DFT) with Koopmans's theorem in order to assign the experimental spectra. We describe a new method for predicting the intensity of the photoelectron spectra on the basis of the DFT orbitals.

Experimental Section

Reactions and manipulations were carried out under an atmosphere of dry nitrogen, either in a Vacuum Atmospheres drybox or using standard Schlenk techniques. Solvents were dried (using standard procedures),[7] distilled, and deoxygenated prior to use, unless otherwise indicated. Glassware was oven-dried at 160 °C overnight. ^1H NMR spectra were recorded on a General Electric QE-300 spectrometer. ^{13}C, ^{14}N, and ^{15}N

[†] Du Pont Contribution No. 6866.
[‡] DuPont Science and Engineering Laboratory.
[#] Johann Wolfgang Goethe-Universität.
[|] Cray Research, Inc.
[▲] University of Wisconsin.
[§] Oxford University.
[⊥] Technischen Universität München.
[⊛] Abstract published in *Advance ACS Abstracts,* July 1, 1994.
(1) Arduengo, A. J., III; Harlow, R. L.; Kline, M. *J. Am. Chem. Soc.* **1991,** *113,* 361.
(2) Arduengo, A. J., III; Dias, H. V. R.; Harlow, R. L.; Kline, M. *J. Am. Chem. Soc.* **1992,** *114,* 5530.
(3) Arduengo, A. J., III; Dias, H. V. R.; Dixon, D. A.; Harlow, R. L.; Klooster, W. T.; Koetzle, T. F. *J. Am. Chem. Soc.* **1994,** *116,* 6812.
(4) Arduengo, A. J., III; Dixon, D. A.; Kumashiro, K. K.; Lee, C.; Power, W. P.; Zilm, K. W. *J. Am. Chem. Soc.* **1994,** *116,* 6361.
(5) Denk, M.; Lennon, R.; Hayashi, R.; West, R.; Belyakov, A. V.; Verne, H. P.; Haaland, A.; Wagner, M.; Metzler, N. *J. Am. Chem. Soc.* **1994,** *116,* 2691.
(6) Herrmann, W. A.; Denk, M.; Behm, J.; Scherer, W.; Klingan, F.-R.; Bock, H.; Solouki, B.; Wagner, M. *Angew. Chem., Int. Ed. Engl.* **1992,** *11,* 1485.

(7) Perrin, D. D.; Armarego, W. L. F.; Perrin, D. R. *Purification of Laboratory Chemicals;* Pergamon: New York, 1985.

NMR spectra were recorded on a GE Omega 300WB spectrometer. NMR references are $(CH_3)_4Si$ (^1H, ^{13}C) and $NH_4^+NO_3^-$ (^{15}N). Melting points were obtained on a Thomas-Hoover capillary apparatus and were not corrected. Elemental analyses were performed by Oneida Research Services, Whitesboro, NY. The photoelectron (PE) spectra were measured using a PES Laboratories 0078 photoelectron spectrometer which has a hollow cathode He discharge lamp capable of providing both He I and He II radiation. The sample of **1a** was held at room temperature external to the spectrometer, whereas the samples of **1b** and **1c** were held at temperatures between 40 and 46 °C for data collection. Data were collected by repeated scans on an Atari microprocessor. The spectra were calibrated with reference to N_2, Xe, and He.

Synthesis of 1,3-Di-*tert*-butylimidazol-2-ylidene (1a). Under an inert atmosphere, a round-bottomed flask was charged with 5 g (23.3 mmol) of 1,3-di-*tert*-butylimidazolium chloride (prepared by established procedures[8]) and 50 mL of THF. The mixture was stirred at 23 °C and 2.8 g (24.9 mmol) of potassium *tert*-butoxide was added in a single portion. The reaction was stirred for 30 min. The mixture was filtered through a Celite mat. The filter cake was washed with 20 mL of THF. The filtrate was concentrated in vacuo to afford 3.5 g of the crude **1a**, yield 84% of theory. The solid was recrystallized by cooling a hexane solution. NMR spectra: ^1H (THF-d_8) δ 1.46 (s, 18H, *t*-Bu), 6.99 (s, 2H, NCCH); ^{13}C (THF-d_8) δ 31.60 (s, CH_3), 56.07 (s, CC_3), 115.44 (s, NCCN), 213.20 (s, NCN); ^{15}N (THF-d_8) δ –164.10. Anal. Calcd for $C_{11}H_{20}N_2$: C, 73.28; H, 11.18; N, 15.54. Found: C, 73.32; H, 10.97; N, 15.54.

Preparation of 1b and 1c. The silylene and germylene compounds (**1b** and **1c**) were prepared according to established procedures.[5,6]

X-ray Crystal Structure of 1,3-Di-*tert*-butylimidazol-2-ylidene (1a). Formula $C_{11}H_{20}N_2$; orthorhombic; space group *Pbca* (No. 61); a = 1162.8-(4), b = 1731.4(6), c = 1135.4(5) pm; T = –100 °C; Z = 8; FW = 180.29; D_c = 1.048 g cm^{-3}; μ(Mo) = 0.58 cm^{-1}; crystal description, colorless flat needle (0.18 × 0.11 × 0.48 mm^3) grown by cooling a hexamethyldisiloxane solution of **1a**. A total of 2318 reflections was collected, 4.2° ≤ 2θ ≤ 50.0°, data octants + – +, ω scan method, scan width = 1.20°ω, scan speed = 2.90–11.70 deg min^{-1}, on a Syntex R3 diffractometer with graphite monochromator using Mo K_α radiation (λ = 71.073 pm), typical half-height peak width = 0.31°ω, two standards collected 28 times, adjusted for a 3% decrease in intensity, no absorption correction. With 700 unique reflections of intensity greater than 2.5σ, the structure was solved by direct methods (MULTAN) and refined by full-matrix least squares on F with scattering factors from the International Tables for X-ray Crystallography, Vol. IV, and weights ∝ $[\sigma^2(I) + 0.0009I^2]^{-1/2}$. The asymmetric unit consisted of one carbene molecule in a general position. Hydrogen atoms idealized with r_{C-H} = 95 pm. There were 118 parameters (data/parameter ratio = 5.93) with all non-hydrogen atoms anisotropic and all hydrogens in fixed positions. The final R factors were R = 0.062 and R_w = 0.054. The error of fit was 1.35, max Δ/σ = 0.00. The final difference Fourier showed the largest residual density to be 0.25 e Å^{-3}, background. Further details of the crystal structure are available in the supplementary material.

Computations

The density functional theory[9-13] calculations were done with the program DGauss,[14-17] which employs Gaussian basis sets on a Cray YMP computer. The basis sets for carbon and nitrogen are triple-ζ in the valence space augmented with a set of polarization functions with the form (7111/411/1).[18] For hydrogen, a polarized triple-ζ valence basis

set was used with the form (311/1). For silicon a polarized triple-ζ valence basis set of the form (73111/6111/1) was used, and for germanium a polarized double-ζ valence basis set of the form (633321/5321/41) was used. The calculations were done at the self-consistent gradient-corrected (nonlocal) level (NLDFT) with the nonlocal exchange potential of Becke[19-21] together with the nonlocal correlation functional of Perdew[22] (BP). The local potential of Vosko, Wilk, and Nusair[23] was used. Geometries were optimized by using analytical gradients.[14-17]

Results

Geometries. The series of compounds **1a–c** shows a smooth structural change as the two-coordinate center is changed from carbon to silicon to germanium. The N–E (E = C, Si, Ge) bond distances increase, and the N–E–N angle steadily decreases (Table 1). These structural trends are reproduced reasonably well by the DFT calculations (Table 1). The silylene and germylene were optimized in the local minimum with the *tert*-butyls staggered (as found for the carbene), since this provides an averaged environment for the two-coordinate main group IV center.

Photoelectron spectra: Experimental Results. The He I PE spectra of the three compounds are given in Figure 1. Ionization energies (IEs) are given in Table 2. The PE spectra differ significantly in the low-IE region (below 11 eV). The broad complex band centered around 12.5 eV contains ionizations of electrons from orbitals with large contributions from the *tert*-butyl groups. The broadening in this region of the experimental spectra is likely to be the result of motional averaging. For the most part this high-energy region is similar in profile for the three compounds, including the presence of a shoulder on the low-IE edge at 11.21 eV for **1a**, 10.76 eV for **1b**, and 10.55 eV for **1c**. The He II PE spectra of the three compounds are given in Figure 2 and show the same bands but somewhat varied intensities, as discussed below.

The PE spectrum of **1a** (Figure 2a) contains three bands in the IE region below 10.5 eV, but in this case the first two bands overlap. Little relative intensity change is observed on change of the ionizing radiation (Table 3).

The PE spectrum of **1b** (Figure 1c) shows three separate bands, A–C, at low ionization energy (IE). The second band B, at 8.21 eV, is the least intense (Table 3), and band C is the most intense. This difference in intensities is exaggerated in the He II spectrum (Figure 2c). The first band shows clear vibrational structure (Figure 3) with three identifiable components separated by 0.16 eV which can be tentatively assigned to a stretching frequency of the molecular ion in its ground state of 1291 ± 15 cm^{-1}.

Table 1. Comparison of Theoretical and Experimental Selected Bond Lengths (pm) and Angles (deg) in **1a–c**[a,b]

	1a		1b		1c	
property	expt	theor	expt[c]	theor	expt[d]	theor
$r(E_2-N_{1(3)})^e$	136.2	137.6	175.3(5)	179.8	185.9	191.8
$r(C_4-C_5)$	134.1(2)	136.2	134.7(21)	136.3	136.4	136.8
$r(N_{1(3)}-C_{5(4)})$	138.7	139.7	140.0(9)	138.9	138.4	137.9
$r(N_{1(3)}-t-Bu)$	145.2	149.8		149.7	149.3	149.2
$\theta(N_1-E_2-N_3)$	102.2(5)	102.4	90.5(10)	86.5	84.8	83.0
$\theta(C_{5(4)}-N_{1(3)}-E_2)$	112.6	112.5		113.3	113.3	113.3
$\theta(N_{1(3)}-C_{5(4)}-C_{4(5)})$	106.3	106.3	114.1(5)	113.4	114.9^f	115.2
$\theta(E_2-N_{1(3)}-t-Bu)$	125.0	123.0		125.3	126.1	125.2

[a] The numbering scheme for all compounds is as indicated for **1a**. [b] Chemically equivalent positions have been averaged. [c] From electron diffraction, see ref 5. [d] From ref 6. [e] E = C, Si, or Ge. [f] This angle was misprinted in ref 6.

(8) Arduengo, A. J., III. U.S., Patent 5182405, 1993.

(9) Parr, R. G.; Yang, W. *Density Functional Theory of Atoms and Molecules*; Oxford University Press: New York, 1989.

(10) Salahub, D. R. In *Ab Initio Methods in Quantum Methods in Quantum Chemistry*; Lawlwy, K. P., Ed.; J. Wiley & Sons: New York, 1987; Vol. II, p 447.

(11) Wimmer, E.; Freeman, A. J.; Fu, C.-L.; Cao, P.-L.; Chou, S.-H.; Delley, B. *Supercomputer Research in Chemistry and Chemical Engineering*; ACS Symposium Series 353; American Chemical Society: Washington, DC, 1987.

(12) Jones, R. O.; Gunnarsson, O. *Rev. Mod. Phys.* **1989**, *61*, 689.

(13) Zeigler, T. *Chem. Rev.* **1991**, *91*, 651.

(14) Andzelm, J. W.; Wimmer, E.; Salahub, D. R. *The Challenge of d and f Electrons: Theory and Computation*; ACS Symposium Series 394; American Chemical Society: Washington, DC, 1989.

(15) Andzelm, J. W. *Density Functional Methods in Chemistry*; Springer-Verlag: New York, 1991.

(16) Andzelm, J. W.; Wimmer, E. *J. Chem. Phys.* **1992**, *96*, 1280.

(17) DGauss is a density functional program available via the Cray Unichem Project.

(18) Godbout, N.; Salahub, D. R.; Andzelm, J. W.; Wimmer, E. *Can. J. Chem.* **1992**, *70*, 560.

(19) Becke, A. D. *Phys. Rev. A* **1988**, *38*, 3098.

(20) Becke, A. D. *The Challenge of d and f Electrons: Theory and Computation*; ACS Symposium Series 394; American Chemical Society: Washington, DC, 1989.

(21) Becke, A. D. *Int. J. Quantum Chem., Quantum. Chem. Symp.* **1989**, *23*, 599.

(22) Perdew, J. P. *Phys. Rev. B* **1986**, *33*, 8822.

(23) Vosko, S. J.; Wilk, L.; Nusair, M. *Can. J. Phys.* **1980**, *58*, 1200.
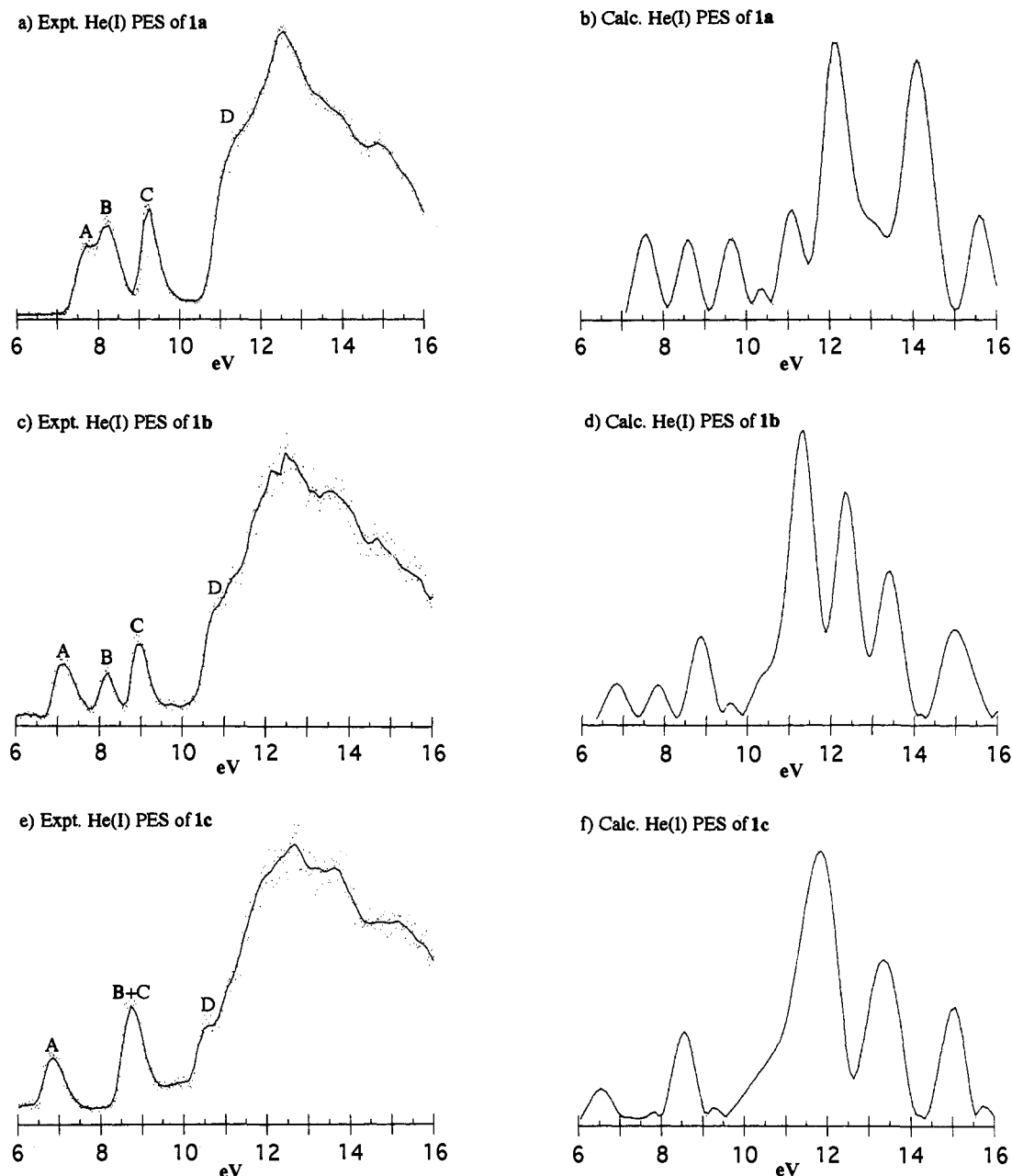
Figure 1. Experimental and calculated He I PE spectra of **1a–c**. The calculated spectra have been shifted so that the lowest ionization energy bands correspond to the experimental values.

Table 2. Ionization energies (eV) in the PE spectra of **1a–c**

band	compound		
	1a	**1b**	**1c**
A	7.68	6.96, 7.13, 7.28	6.65, 6.85, 6.97
B	8.22	8.21	8.60
C	9.24	8.92	8.80
D	11.21	10.76	10.55
	(11.27)[a]	11.27	11.12
	12.55	12.48	12.68
	14.90	13.67	14.96

[a] Position estimated from calculated results.

The PE spectrum of **1c** shows only two bands in the low-IE region. Of these the higher IE band decreases in relative intensity in the He II spectrum (Table 3). The He I relative intensities, when compared to those of compounds **1a** and **1b** suggest that the second band comprises two ionizations. Though two maxima, at 8.60 and 8.80 eV, are observed for this band (Figure 3), their separation could well be attributed to a vibrational progression and cannot be taken as hard evidence for the presence of two

primary ionizations but may well be attributable to this (vide infra). Fine structure is evident in band A (Figure 3).

Photoelectron Spectra: DFT Results. The intensities of the photoelectron spectral bands are calculated by standard first-order time-dependent perturbation theory from the DFT wave function. The initial state consists of the photon plane wave $\exp(-i\mathbf{k}\cdot\mathbf{r})$, with incident direction $\mathbf{n} = \mathbf{k}/k$ and energy $\omega = ck$, and a bound initial electronic state $u_i(\mathbf{r})$, with energy ϵ_i. In the single-particle approximation, the bound state is taken as an occupied Kohn–Sham orbital. In the final state, the photon is absorbed by the system and an electron is ejected. The outgoing electronic state is approximated by a plane wave $u_f(\mathbf{r}) = \exp(-i\mathbf{k}_f\cdot\mathbf{r})$, which should be a good approximation when the photon energy ω is much larger than the absolute value of the initial electron energy ϵ_i. The outgoing electron's energy is fixed by the energy conservation, $\hbar^2 k_f^2/2m = \hbar\omega + \epsilon_i$. The differential cross section for the single-particle state is given in eq 1,[24,25]

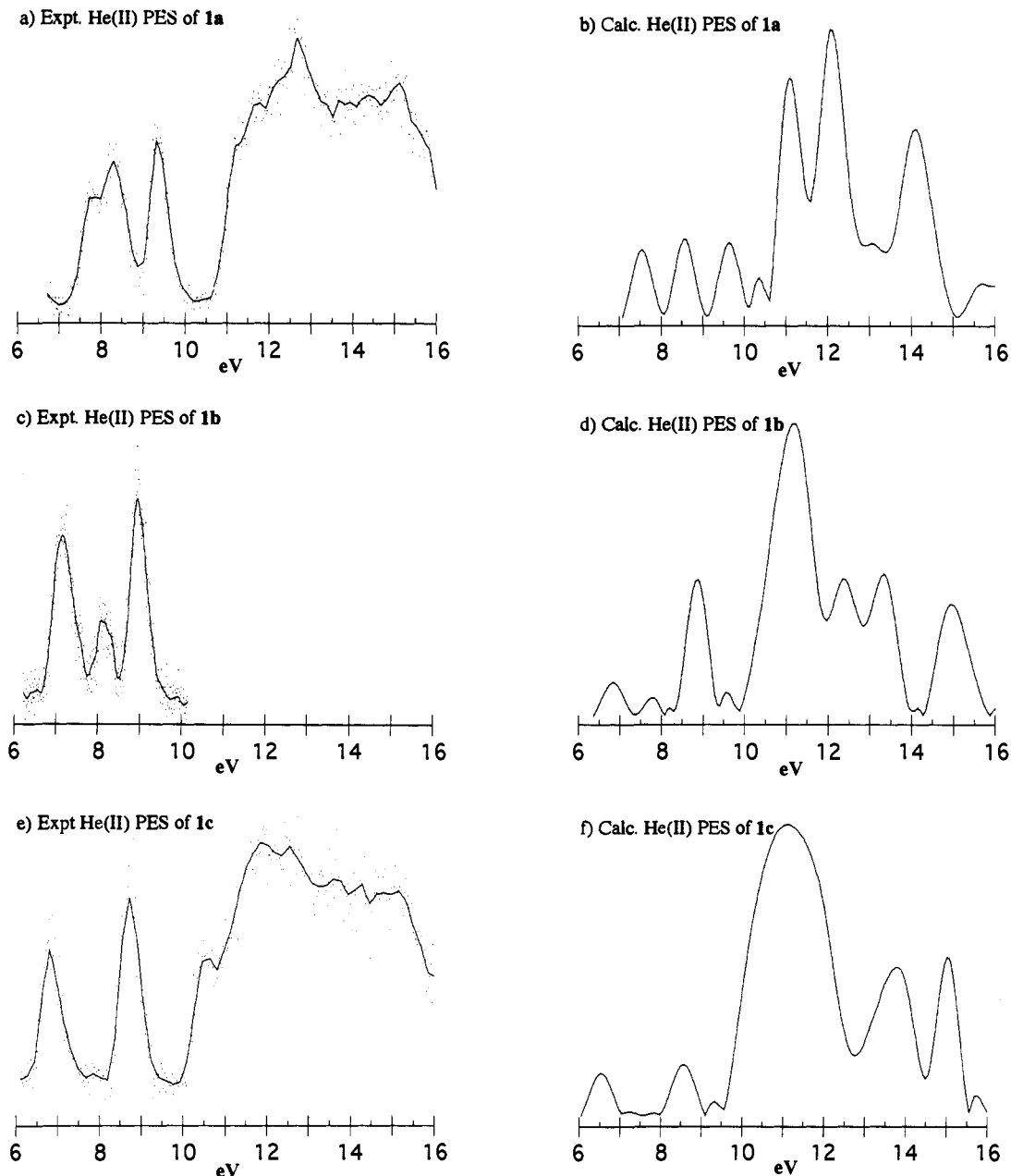(24) Merzbacher, E. *Quantum Mechanics*; John Wiley and Sons, Inc.: New York, 1970.

a) Expt. He(II) PES of **1a**

b) Calc. He(II) PES of **1a**

c) Expt. He(II) PES of **1b**

d) Calc. He(II) PES of **1b**

e) Expt He(II) PES of **1c**

f) Calc. He(II) PES of **1c**

Figure 2. Experimental and calculated He II PE spectra of **1a–c**. The calculated spectra have been shifted so that the lowest ionization energy bands correspond to the experimental values.

Table 3. Relative Intensities of the PE Bands in **1a–c**[a]

compound (source)	band		
	A	B	C
1a			
He I	61 (A + B) (67)		39 (33)
He II	60 (A + B) (66)		40 (34)
1b			
He I	36 (23)	21 (22)	43 (55)
He II	41 (19)	19 (11)	40 (70)
1c			
He I	31 (27)	69 (B + C) (73)	
He II	39 (46)	61 (B + C) (54)	

[a] Numbers in parentheses are the theoretically calculated intensities.

where *F* is an unspecified constant which can be taken as unity as only the line shape of the photoelectron spectrum is of interest here. P_{if} is the transition matrix defined by eq 2 where $\mathbf{q} = \mathbf{k}_f - (\omega/c)\mathbf{n}$. The non-angular-resolved PE spectrum is calculated

(25) Mintmire, J. W.; Kutzler, F. W.; White, C. T. *Phys. Rev. B* **1989**, *36*, 3312.

by integrating over the solid angles $d\Omega$ of eq 1 to obtain the contribution to the total cross section from the *i*th state (eq 3).

$$\frac{d\sigma_i(\omega)}{d\Omega} = F\frac{k_f}{\omega}|P_{if}|^2 \qquad (1)$$

$$P_{if} = \int d^3r\, u_i(r)\nabla \exp(-i\mathbf{q}\cdot\mathbf{r}) \qquad (2)$$

$$\sigma_i(\omega) = \frac{k_f}{\omega}\int d\Omega |P_{if}|^2 \qquad (3)$$

The solid angle integration is performed numerically using 18 quadrature points. The matrix elements P_{if} involve Fourier transformations of Gaussian functions and are calculated analytically. Had we neglected the directional effect of the incident photon $(\omega/c)\mathbf{n}$, as was done previously in the work of Mintmire *et al.*,[25] all of the integrations could be readily evaluated analytically. However, for large ω, the ideal situation where the outgoing electron can be approximated by the plane wave, the term $(\omega/c)\mathbf{n}$ is not negligible.
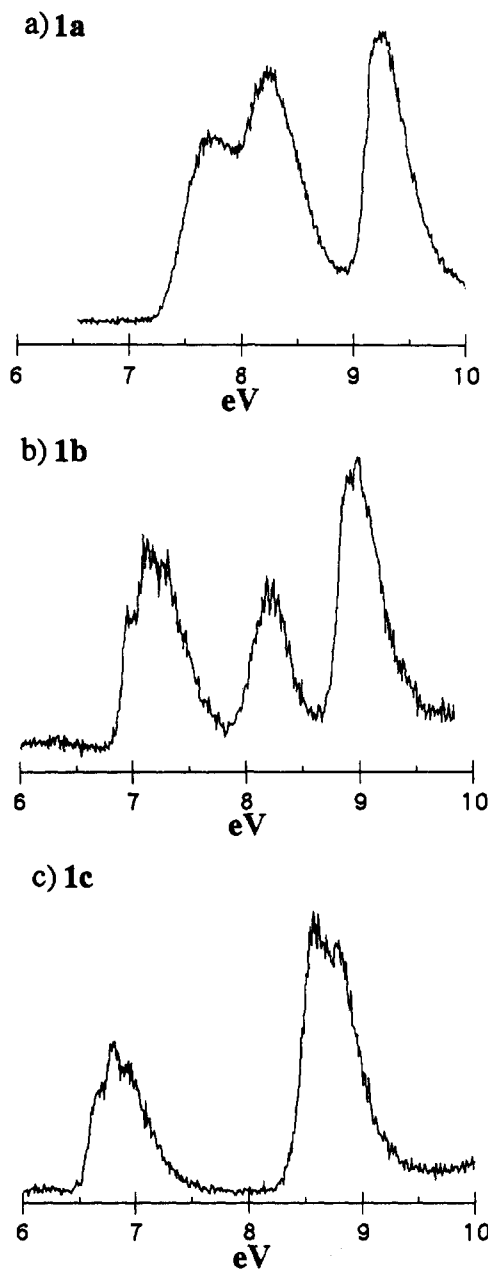
a) 1a

b) 1b

c) 1c

Figure 3. High-resolution He I PE spectra of 1a–c.

Because the experiments cannot distinguish between the initial electronic states, the measured PE spectrum is a summation over all of the contributing initial states (eq 4). Gaussian broadening as represented by Δ is used in place of a δ-function to ensure energy conservation. The Gaussian line width was taken as 0.2 eV after calculations at $\Delta = 0.5$ eV showed too much broadening.

$$\sigma_{tot}(E) = \frac{1}{\Delta\sqrt{\pi}}\sum \exp\left(-\left(\frac{E-\omega-\epsilon_i}{\Delta}\right)^2\right)\sigma_i(\omega) \qquad (4)$$

In DFT, the relationship between the eigenvalue ϵ_i and the total energy E_{tot} is given by the Janak relation (eq 5).[26]

$$\epsilon_i = dE_{tot}/dn_i \qquad (5)$$

In order to apply an approximate version of Koopmans's theorem[27] at the DFT level, one has to assume that ϵ_i is independent of the occupation number n_i. Slater's transition-state formula[9,28,29]

(26) Janak, J. F. *Phys. Rev. B* **1978**, *18*, 7165.
(27) Koopmans, T. *Physica* **1934**, *1*, 104.
(28) Slater, J. C. *Adv. Quantum Chem.* **1972**, *6*, 1.

Table 4. Calculated PE spectra and Assignments of 1a–c[a]

1a		1b		1c	
energy[b]	assignment	energy[c]	assignment	energy[d]	assignment
7.68	C σ-lp	6.96	π-3	6.65	π-3
8.46	π-3	8.01	Si σ-lp	8.36	Ge σ-lp
9.53	π-2	8.85	π-2	8.69	π-2
11.15	σ-t-Bu	10.38	σ-t-Bu + Si–N	10.08	σ-Ge–N
11.21	π-1 + σ-t-Bu	10.60	π-1 + σ-t-Bu	10.47	π-1 + σ-t-Bu
11.29	σ	10.82	σ	10.76	σ
11.46	σ	10.96	σ	10.87	σ

[a] Energy in eV. [b] Calculated orbital energies shifted by 3.14 eV. [c] Calculated orbital energies shifted by 2.57 eV. [d] Calculated orbital energies shifted by 2.48 eV.

for the molecular ionization potential (IP) for a system of N electrons (which can be generalized to any ϵ_i) is given by eq 6.

$$-IP = E_N - E_{N-1} = \int_0^1 \epsilon_{HOMO}(n)\, dn \qquad (6)$$

One approximation is that the integral can be approximated by the value of ϵ_i for $n_i = {}^1/_2$. In the PE spectral calculation as described above, one does not really need for ϵ_i to stay independent of n_i as long as ϵ_i changes by the same amount for all of the eigenvalues in the region of interest when n_i changes. This assumption is borne out by the comparison in Figure 1. Further, this constraint may not be as important at the nonlocal DFT level that we have used as opposed to the local DFT level because the correction to the exchange potential[19-21] that we use accounts for part of the self-interaction correction missing at the local level.[30] It is this self-interaction term that leads to the dependence of ϵ_i on n_i. Furthermore, the absolute calculated values are not as critical, as we are going to apply a uniform shift based on the difference in the calculated and experimental molecular ionization potentials in order to directly compare the orbital energies to experiment.

The calculated photoelectron spectra are shown in Figures 1 and 2 for initial photoelectron energies of 21.2 and 40.8 eV, which correspond to the He I and He II lines. The calculated ionization energies have been shifted so that the first ionization energies correspond to those observed in the experimental spectra. The calculated IEs and assignments are given in Table 4.

These results can be used to assign the photoelectron spectra. The calculations show three clearly resolved peaks of about equal intensity. For the carbene 1a, the HOMO is unambiguously the in-plane lone pair on the carbene carbon, as depicted in Figure 4a (henceforth called σ-lp). This σ-lp orbital is responsible for band A at 7.68 eV. The next two bands arise from π-orbitals of the imidazole group as shown in Figure 4d and g. The π-orbital depicted in Figure 4d (henceforth called π-3) is largely the C=C π-orbital with some out-of-phase mixing of the nitrogen lone pairs and carbene p-orbital. The π-3 orbital gives rise to band B at 8.22 eV. The π-orbital depicted in Figure 4g is essentially the out-of-phase combination of the nitrogen lone pairs (henceforth called π-2) and gives rise to band C at 9.24 eV. Band D begins a group of ionizations from largely σ-orbitals. The band at 11.21 eV is due to the σ-orbital depicted in Figure 4j. This σ-orbital primarily represents *tert*-butyl C–C bonds but does show some mixing with the imidazole ring σ-bonds. Just below this level ($\Delta E = 0.061$ eV) is a $\sigma+\pi$-orbital (not illustrated in Figure 4) which is comprised of the all-in-phase π-1 orbital in the imidazole ring and *tert*-butyl σ-bonds which are antisymmetric with respect to the molecular plane. This very close π-1 level undoubtedly also contributes to the shoulder band D.

For the silylene derivative 1b, again there are three low-energy bands with the third band predicted to have somewhat more

(29) Slater, J. C. *The Self Consistent Field for Molecules and Solids: Quantum Theory of Molecules and Solids*; McGraw-Hill: New York, 1974.
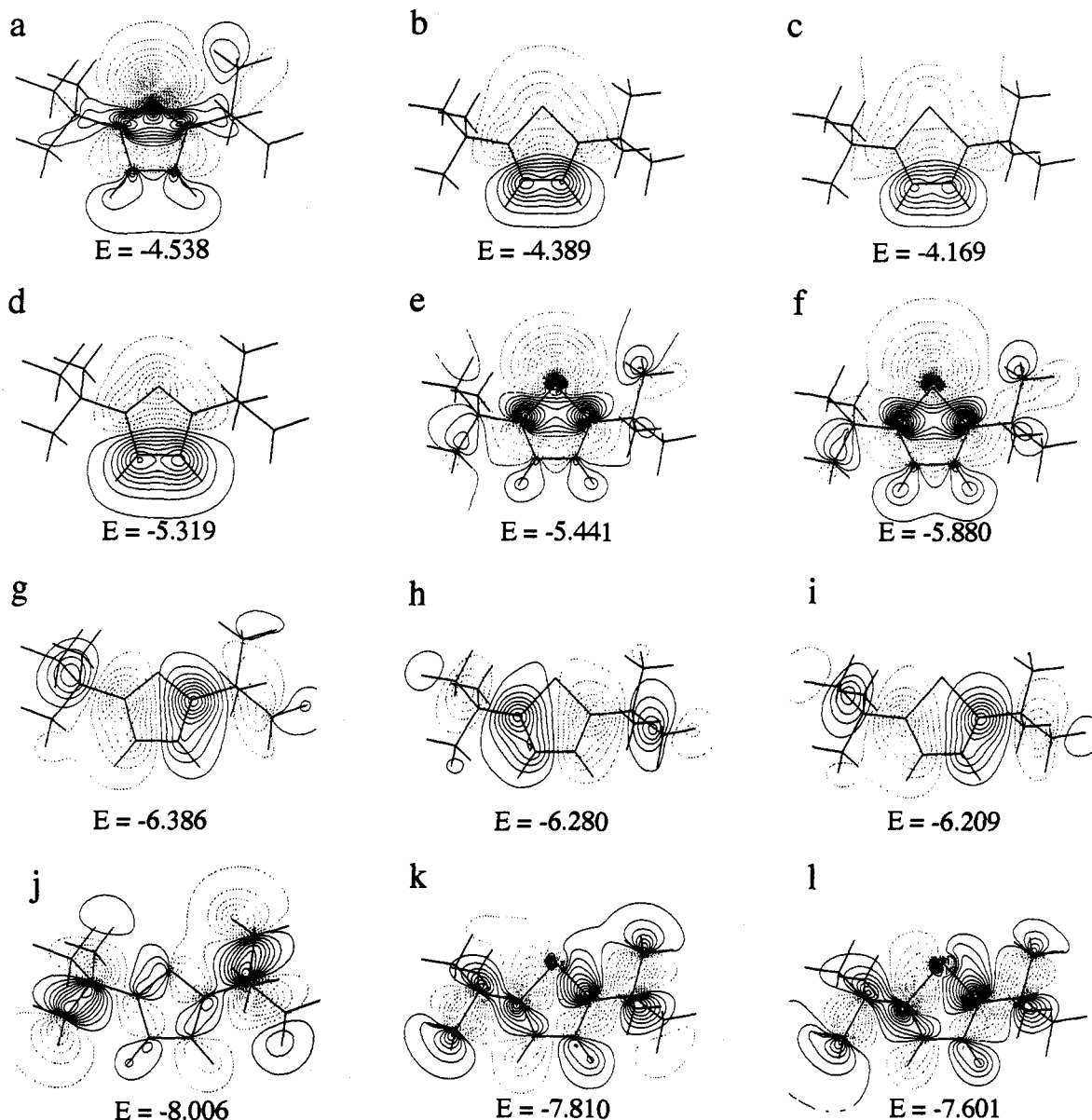(30) Perdew, J. P.; Zunger, A. *Phys. Rev. B* **1981**, *23*, 5048.

6646   *J. Am. Chem. Soc., Vol. 116, No. 15, 1994*

Arduengo et al.

a

E = -4.538

b

E = -4.389

c

E = -4.169

d

E = -5.319

e

E = -5.441

f

E = -5.880

g

E = -6.386

h

E = -6.280

i

E = -6.209

j

E = -8.006

k

E = -7.810

l

E = -7.601

Figure 4. Various DFT calculated molecular orbitals in **1a–c**. Orbitals b, c, d, g, h, and i are π-orbitals that are represented by a single contour plane 70 pm above the molecular plane. The orbitals a, e, and f are the σ-lp orbitals. Orbitals b, c, and d are the orbitals designated as π-3. The π-2 orbitals are depicted in g, h, and i. Carbene orbitals are a, d, g, and j. Silylene orbitals are b, e, h, and k. Germylene orbitals are c, f, i, and l.

intensity than the first two, in excellent accord with the experimental spectrum. The calculations unambiguously assign the HOMO to π-3 for band A at 6.96 eV. The drawing of π-3 in **1b** (Figure 4b) shows a similar structure to that of the analogous orbital in **1a** (Figure 4d) except that the C=C π-bond contribution is diminished and the contribution from silicon is enhanced. Band B at 8.21 eV now has its origins in the silicon σ-lp. This ordering for bands A and B is reversed from that for the carbene. Band C is again due to the out-of-phase N-lone pairs (π-2) and is similar in structure (Figure 4h) and energy to the corresponding orbital in the carbene. The shoulder band D at 10.76 eV in **1b** is again due to a σ-bonding orbital that now has substantial contributions from the Si–N σ-bonds in the ring. The nearby σ + π-1 orbital which was a contributor to band D in **1a** is now further separated at (ΔE = 0.222 eV) and may be evident as a slight second shoulder in the experimental PE spectrum (Figure 1c).

The germylene derivative **1c** exhibits only two low-energy bands in the experimental spectrum (Figure 1e). The calculated spectrum (Figure 1f) also shows two moderately intense low-energy bands. As in the silylene derivative, the HOMO band A at 6.65 eV is the π-3 orbital that has a continuing diminution of

the C–C π-bond component relative to the case of **1b** (vide supra). The second band at ~8.7 eV is actually a combination band, B + C (Figure 4b) with contributions from the closely spaced σ-lp and π-2 orbitals (ΔE = 0.329 eV). The shoulder band D at 10.55 eV is again due to a σ-orbital that has now become primarily the out-of-phase combination of the two Ge–N bonds with some contributions from the C–C bonds of the *tert*-butyls (Figure 4l). The subjacent σ + π-1 orbital is now further removed into the broad high-energy bands (ΔE = 0.393 eV).

Discussion

The experimental trend in the first ionization energy (band A) is a decrease in the energy with increasing atomic number, with Δ(C–Si) = 0.72 eV and Δ(Si–Ge) = 0.31 eV. The calculated values (unshifted, see Figure 4) show the same trend but with smaller magnitudes with Δ(C–Si) = 0.15 eV and Δ(Si–Ge) = 0.22 eV. Band B is predicted to have the opposite trend, with the heavier atomic numbers leading to a larger ionization energy. Experimentally band B is about the same for the carbene and silylene but significantly higher for the germylene. The calculations reproduce the order for the third ionization energy, which corresponds to the π-2 orbital. To facilitate the comparison of

A Carbene/Silylene/Germylene Series

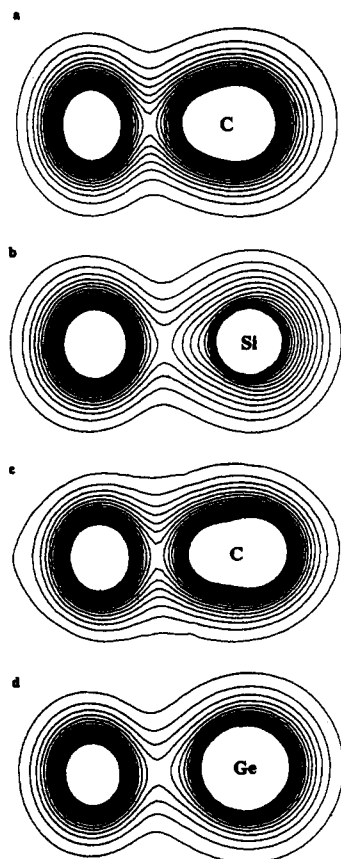*J. Am. Chem. Soc., Vol. 116, No. 15, 1994* 6647

Figure 5. Electron density in a plane orthorgonal to the molecular plane that bisects the C=C double bond and the two-coordinate main group IV center. The two-coordinate main group IV center is to the right and the C=C bond is on the left of each drawing. The contours are drawn from the total electron density between 0.05 and 1.0 e Å^{-3} at 0.05 intervals. (a) DFT calculated density in **1a**. (b) DFT calculated density in **1b**. (c) Experimentally determined density in 1,3,4,5-tetramethylimidazol-2-ylidene-d_{12} (see ref 3). (d) DFT calculated density in **1c**.

the experimental and theoretical results, the calculated spectra were shifted from the raw orbital energies calculated at the DFT level (Figure 4). Since any such shift is somewhat arbitrary, we chose to shift the calculated values so that the energies of band A would be in agreement between theory and experiment (Table 4).

On the basis of the assignments, the trends in the ionization energies of the various orbitals can be evaluated. The ionization energy of the two-coordinate main group IV center lone pair (σ-lp) increases as the atomic number increases. The overall structure of this σ-lp orbital is similar in the three compounds (Figure 4a, e, and f). In contrast the ionization energy of an electron from the π-3 orbital decreases with increasing atomic number at the two-coordinate main group IV center. Additionally, the structure of the π-3 orbital changes between the three compounds. In the carbene **1a**, the π-3 orbital is comprised of a large component from the C=C double bond in the imidazole ring. The relative contribution of the C=C double bond decreases as the atomic number of the two-coordinate main group IV center increases. This results in changes in π-3 that localize more electron density onto the two-coordinate main group IV center.

To evaluate the changes in electron distribution at the two-coordinate main group IV centers, we have plotted a diffuse portion of the DFT-predicted total electron density at these centers in Figure 5. The plane of density which has been plotted is orthogonal to the molecular plane and bisects the C=C double bond (*i.e.*, the contoured plane is rotated 90° from the molecular plane about the pseudo two-fold axis that passes through the two-coordinate main group IV center and bisects the C=C double bond). These

plots provide a view of the electron density at the two-coordinate main group IV centers as well as a cross section through the center of the C=C double bond. The carbene center in **1a** is predicted to have an electron distribution which is "egg-shaped" (Figure 5a). This type of electron distribution is characteristic of carbenes such as $^1A_1$ CH_2 and CF_2.[3] For comparison, the experimentally determined electron distribution for 1,3,4,5-tetramethylimidazol-2-ylidene-d_{12} is shown in Figure 5c.[3] The electron distribution predicted for **1a** appears quite similar to that previously found for 1,3,4,5-tetramethylimidazol-2-ylidene-d_{12}. In contrast, the electron distributions around the silicon and germanium centers in **1b** and **1c** appear far more circular (Figure 5b and d). This more symmetrical electron distribution at the heavier two-coordinate main group IV centers is in accord with the changes predicted for the π-3 level. Another observation that should be made from the drawings in Figure 5 is the oval distribution of electrons in the C=C double-bond cross sections (with the long oval axis normal to the molecular plane). This is consistent with the expected σ + π nature of the electron density between these two double bonded carbons.

In contrast to the changes in the σ-lp and π-3 orbitals, the π-2 orbital that is manifested as band C in the PE spectra remains fairly constant in both energy (Tables 2 and 4) and structure (Figure 4g–i) among **1a–c**. Since this orbital is essentially made up of the out-of-phase combination of the out-of-plane nitrogen p-lone pairs and formally has no contribution from the two-coordinate main group IV center, this invariance is expected.

Band D again shows a steady change through the three compounds. The molecular orbital that is responsible for the D band is a σ-orbital that is largely comprised of C–C bonds in the *tert*-butyl groups in **1a**. As the atomic number of the two-coordinate main group IV center is increased, electrons from this orbital become easier to ionize (Tables 2 and 4) and the orbital structure has smaller contributions from the C–C σ-bonds and a larger contribution from the two E–N bonding regions (Figure 4k and l). The actual distribution in the E–N bonding regions is somewhat suggestive of in-plane nitrogen lone pairs of electrons from hypothetical chelation of a main group IV center by a diazabutadiene (*t*-BuDAB) ligand (structure **2**).

Structure **2** is doubtless an extreme exaggeration of the bonding that is developing in **1b** and **1c**. Nonetheless it offers powerful

2 E = Si, Ge
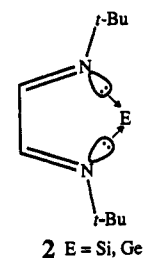
insight into the bonding in these compounds. The increasing importance of the valence bond representation **2** is signaled by the transformations of π-3 that, in the extreme case of complete electron transfer to the two-coordinate main group IV center from the C=C double bond, would result in the development a p-type lone pair of electrons at the heavier two-coordinate main group IV centers. Additionally, the increasing importance of the two N–E bonds in the molecular orbital responsible for band D further supports the growing importance of a valence bond structure like **2** as the atomic number of the two-coordinated main group IV center increases. This transformation is apparent in the predicted electron distribution around the two-coordinate main group IV centers. The total electron density in the molecular planes of **1a–c** again provides clues to the differences among the structures **1a–c**. Figure 6 illustrates the electron density in the molecular planes of **1a–c** (Figure 6a, b, and d) as well as a
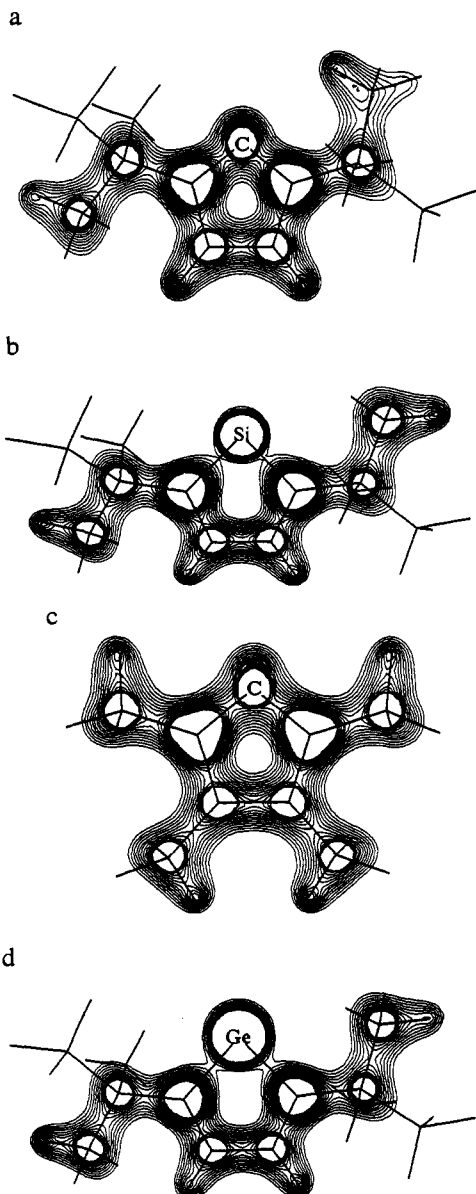
a

b

c

d

Figure 6. Electron density in the molecular plane of **1a–c** and 1,3,4,5-tetramethylimidazol-2-ylidene-d_{12}. The contours are drawn from the total electron density between 0.75 and 3.0 e Å^{-3} at 0.15 intervals. (a) DFT calculated density in **1a**. (b) DFT calculated density in **1b**. (c) Experimentally determined density in 1,3,4,5-tetramethylimidazol-2-ylidene-d_{12} (see ref 3). (d) DFT calculated density in **1c**.

comparison to the experimentally determined electron distribution in 1,3,4,5-tetramethylimidazol-2-ylidene-d_{12} (Figure 6c). For the carbene compounds, typical σ-bonds are found throughout the imidazole ring and for the attached groups. In contrast, the DFT-predicted electron distributions for the silicon- and germanium derived compounds reveal somewhat isolated circular electron distributions about these heavier two-coordinate main group IV centers whereas the other ring σ-bonds remain unchanged. The circular in-plane electron density at germanium and silicon in conjunction with the circular electron density normal to the molecular plane (Figure 5) leads to an essentially spherical distribution of electron density around these heavier main group IV centers. This spherical electron distribution underscores the "chelated atom" nature of the bonding in **1b** and **1c** as depicted in structure **2**.

The spherical distribution of electron density around the silicon and germanium centers in **1b** and **1c** should lead to some substantial differences in chemistry relative to the carbene **1a**. Complexes of substituted analogs of the carbene, silylene, and

germylene have been reported and can be described by structure **3**, in which a single σ-lone pair of electrons from the two-coordinate main group IV center is donated to a Lewis acid (main group or transition metal centered).[6,31–40]

E = C, Si, Ge
L.A. = Lewis acid
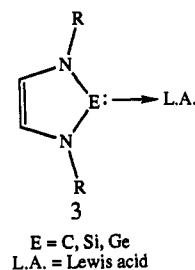
The higher, more spherical electron distribution and the increasing π-lone pair character of the π-3 orbital that is actually the HOMO for the silicon and germanium compounds suggests that these compounds might also serve as four-electron donors. Indeed, if the t-BuDAB ligand in **1b** and **1c** is replaced by α,α'-bipyridyl, such complexes are known for germanium, tin, and lead (**4**).[41,42] In complexes such as structure **4** the central main

E = Ge, Sn, Pb
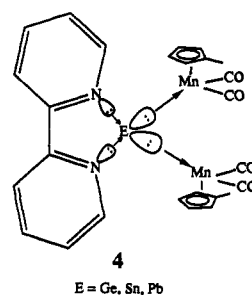
group IV center is actually four-coordinate and tetrahedral rather than three-coordinate and trigonal-planar as in **3**. For silicon, a remarkable example of such bonding has been reported, as shown in structure **5**, in which the nucleophiles coordinated to the silicon center come from two discrete HMPA molecules rather than from a single bidentate ligand.[43]

5
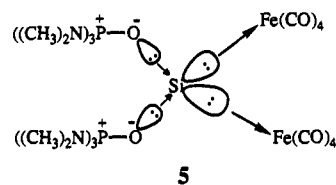
(31) Arduengo, A. J., III; Kline, M.; Calabrese, J. C.; Davidson, F. *J. Am. Chem. Soc.* **1991**, *113*, 9704.

(32) Arduengo, A. J., III; Dias, H. V. R.; Calabrese, J. C.; Davidson, F. *J. Am. Chem. Soc.* **1992**, *114*, 9724.

(33) Arduengo, A. J., III; Dias, H. V. R.; Calabrese, J. C.; Davidson, F. *Inorg. Chem.* **1993**, *32*, 1541.

(34) Arduengo, A. J., III; Dias, H. V. R.; Davidson, F.; Harlow, R. L. *J. Organomet. Chem.* **1993**, *462*, 13.

(35) Arduengo, A. J., III; Dias, H. V. R.; Calabrese, J. C.; Davidson, F. *Organometallics* **1993**, *12*, 3405.

(36) Arduengo, A. J., III; Gamper, S. F.; Calabrese, J. C.; Davidson, F. *J. Am. Chem. Soc.* **1994**, *116*, 4391.

(37) Arduengo, A. J., III; Tamm, M.; Calabrese, J. C. *J. Am. Chem. Soc.* **1994**, *116*, 3625.

(38) Kuhn, N.; Henkel, G.; Kratz, T.; Kreutzberg, J.; Boese, R.; Maulitz, A. H. *Chem. Ber.* **1993**, *126*, 2041.

(39) Kuhn, N.; Henkel, G.; Kratz, T. *Chem. Ber.* **1993**, *126*, 2047.

(40) Kuhn, N.; Kratz, T.; Henkel, G. *J. Chem. Soc. Chem. Commun.* **1993**, 1778.

(41) Ettel, F.; Huttner, G.; Zsolnai, L. *Angew. Chem., Int. Ed. Engl.* **1989**, *28*, 1496.

(42) Ettel, F.; Huttner, G.; Imhof, W. *J. Organomet. Chem.* **1990**, *397*, 299.

(43) Zybill, C.; Wilkinson, D. L.; Muller, G. *Angew. Chem., Int. Ed. Engl.* **1988**, *27*, 583.

A Carbene/Silylene/Germylene Series

J. Am. Chem. Soc., Vol. 116, No. 15, 1994 6649

The synthetic approach to structures 4 and 5 actually employed complexation of the main group IV center by bipyridyl or HMPA after the metal–main group IV bonds were formed so that discrete silylenes, germylenes, stannylenes, and plumbylenes were not involved. Nonetheless their existence points to a key difference between the bonding in **1a** and that in **1b** and **1c** and offers an interesting synthetic challenge for the synthesis of structures like **4** directly from **1b** and **1c**.

Conclusion

The photoelectron spectra of a stable carbene, silylene, and germylene have been recorded. These spectra are accurately simulated by a time-dependent first-order perturbation theory analysis of the density functional theory wave functions for the compounds. The unambiguous assignments of the bands in the photoelectron spectra reveal that the carbene **1a** possesses a σ-lone pair highest occupied molecular orbital at the carbene center. In contrast, the silylene and germylene both possess HOMOs derived from π-orbitals that become more localized on the main group IV center with increasing atomic number. The σ-lone pair orbital falls in energy with increasing atomic number throughout the series **1a–c**, thus producing a rise in ionization energy for electrons from this orbital. There is a π-orbital that is largely comprised of an out-of-phase combination of the nitrogen p-lone pairs of electrons that remains fairly constant throughout the series of compounds (band C). A higher energy band (D) reveals a change in bonding to the two-coordinate main group IV centers in **1a–c**. The changes in orbital energy and structure for **1a–c** predicted by DFT calculations and supported by the experimental photoelectron spectra have provided considerable insight into the electron distribution and potential reactivity of **1a–c**.

The electron distribution at the carbene center is "egg-shaped", showing an excess electron density in the direction of the in-plane σ-lone pair of electrons at the carbene center and a deficit in the direction of the carbene p-π orbital. This deformation is consistent with an experimental determination of the electron density at a related carbene center. The electron distributions at the silicon and germanium centers in **1b** and **1c** are predicted to be essentially spherical and are consistent with structures of metal complexes which emphasize a "chelated atom" analogy for the bonding in **1b** and **1c**. The silylene and germylene structures **1b** and **1c** do not represent simple extensions of the type of bonding in the carbene **1a** but rather begin to assume a degree of zero-valent "chelated atom" character which is reflected in some previously known metal complexes that are related to these structures.

Supplementary Material Available: Cartesian coordinates for the calculated structures of **1a–c**. Tables of fractional coordinates, isotropic and anisotropic thermal parameters, bond distances, and bond angles for **1a**, an ORTEP drawing of **1a**, and text describing the X-ray crystal structure of **1a** (7 pages). This material is contained in many libraries on microfiche, immediately follows this article in the microfilm version of the journal, and can be ordered from the ACS; see any current masthead page for ordering information.